Evaluation of Bioaccumulation Kinetics of Gold Nanorods in Vital Mammalian Organs by Means of Total Reflection X-Ray Fluorescence Spectrometry

ARTICLE *in* ANALYTICAL CHEMISTRY · JULY 2014

Impact Factor: 5.64 · DOI: 10.1021/ac5006475 · Source: PubMed

5 AUTHORS, INCLUDING:

Ramón Fernández Ruiz
Universidad Autónoma de Madrid
53 PUBLICATIONS **514** CITATIONS
SEE PROFILE

Milagros Ramos
Universidad Politécnica de Madrid
26 PUBLICATIONS **495** CITATIONS
SEE PROFILE

analytical chemistry

Article

pubs.acs.org/ac

Evaluation of Bioaccumulation Kinetics of Gold Nanorods in Vital Mammalian Organs by Means of Total Reflection X-Ray Fluorescence Spectrometry

Ramón Fernández-Ruiz,*[,†] María Jesús Redrejo,[†] Eberhardt Josué Friedrich,[†] Milagros Ramos,[‡] and Tamara Fernández[‡]

[†]Servicio Interdepartamental de Investigación, Laboratorio de Fluorescencia de Rayos X por Reflexión Total, Universidad Autónoma de Madrid, 28049 Madrid, Spain

[‡]Centro de Tecnología Biomédica, Universidad Politécnica de Madrid, 28223 Madrid, Spain

ABSTRACT: This work presents the first application of total-reflection X-ray fluorescence (TXRF) spectrometry, a new and powerful alternative analytical method, to evaluation of the bioaccumulation kinetics of gold nanorods (GNRs) in various tissues upon intravenous administration in mice. The analytical parameters for developed methodology by TXRF were evaluated by means of the parallel analysis of bovine liver certified reference material samples (BCR-185R) doped with 10 μg/g gold. The average values (n = 5) achieved for gold measurements in lyophilized tissue weight were as follows: recovery 99.7%, expanded uncertainty (k = 2) 7%, repeatability 1.7%, detection limit 112 ng/g, and quantification limit 370 ng/g. The GNR bioaccumulation kinetics was analyzed in several vital mammalian organs such as liver, spleen, brain, and lung at different times. Additionally, urine samples were analyzed to study the kinetics of elimination of the GNRs by this excretion route. The main achievement was clearly differentiating two kinds of behaviors. GNRs were quickly bioaccumulated by highly vascular filtration organs such as liver and spleen, while GNRs do not show a bioaccumulation rates in brain and lung for the period of time investigated. In parallel, urine also shows a lack of GNR accumulation. TXRF has proven to be a powerful, versatile, and precise analytical technique for the evaluation of GNRs content in biological systems and, in a more general way, for any kind of metallic nanoparticles.

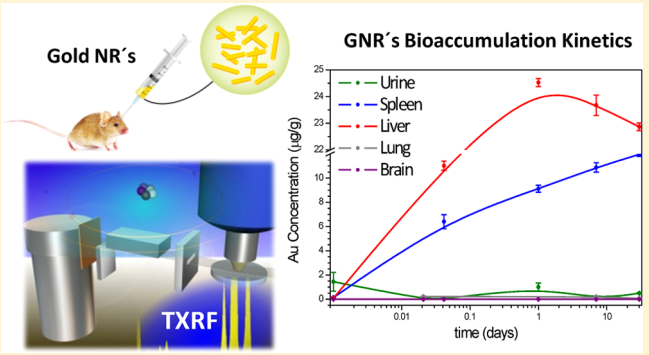

The recent interrelation of nanoparticle technology with potential medical applications is a promising line for treatment and diagnosis of a great variety of diseases. Nanoparticles (NPs) and particularly gold nanoparticles (GNPs) are of great interest for biomedical applications due to their good biocompatibility, high surface areas, nontoxicity, and unique physicochemical properties.[1] GNPs can be easily conjugated to proteins and other molecular species without altering the biological activity of the nanoconjugates.[2] Due to their strong and size-tunable surface plasmon resonance, fluorescence, and easy surface functionalization, gold-based nanomaterials have been widely used in biosensors, cancer cell imaging, photothermal therapy, and drug delivery.[3,4] The increase of nanoparticle applications in biotechnology, medicine, food products, and end consumer products implies that human exposure to this type of nanoparticles will be increased greatly. In this way, it is necessary to investigate carefully the propensity of these nanoparticles to accumulate in the body and produce undesired side effects, both when an environmental exposure to GNPs occurs and when the particles are used for biomedical applications. However, in this work we analyze the bioaccumulation of gold nanorods (GNRs) after a deliberate administration at concentrations typically used for biomedical applications.

The in vivo biodistribution of nanoparticles and its following mechanisms of biodegradation and excretion determine the feasibility and applicability of nanotechnology in the practical clinical translation. Currently, few data and studies are available regarding the long-term accumulation of GNPs, 1 month after their administration in vivo.[5] In most studies, systemically administrated GNRs, like other types of nanoparticles, were primarily taken up by liver and spleen in large quantities, with small amounts distributed in the lung, kidney, heart, and brain at 24−72 h after a single administration.[6−10] Different routes of administration may result in varying effects on the biodistribution pattern of drug carriers.[6] The in vivo distribution of injected NPs largely depends on their particle size and surface properties.[7−10] These studies demonstrated that tissue distribution of gold nanoparticles is size-dependent, with the smallest NPs (10 nm) showing the most widespread organ

Received: February 16, 2014
Accepted: July 7, 2014

   dx.doi.org/10.1021/ac5006475 | *Anal. Chem.* XXXX, XXX, XXX−XXX

distribution, whereas the larger particles (up to 250 nm) were mainly detected in liver and spleen. It has been previously reported that gold nanorods (65 ± 5 nm, 11 ± 1 nm) were accumulated in the liver following intravenous injection with Kupffer cells that play an important role in the elimination of GNPs.[11] However, little is known about the biodistribution and long-term accumulation after 1 month of GNPs administration. Any new contribution in this line should be of great interest for the scientific community related to GNP research.

Characterization of the biodistribution, clearance, and biocompatibility of GNPs used for biomedical applications has an important role in this kind of research, so development of analytical procedures sensitive enough for monitoring and quantifying GNPs, in different kind of tissues, acquires special relevance. In this way, the main achievement of this work is to present an analytical alternative method, total-reflection X-ray fluorescence (TXRF) spectrometry, which has been applied for first time in this kind of GNR research. Additionally, the availability of biological sample, for GNP quantification in these kinds of studies, is usually very low, on the order of a few milligrams. Therefore, only very sensitive techniques such as instrumental neutron activation analysis (INAA)[12] or inductively coupled plasma mass spectrometry (ICP-MS)[13] have been used up to now. An alternative approximation to the low sample availability is the microanalytical capability inherent to TXRF spectrometry, which implies that TXRF can evaluate, at qualitative and semiquantitative levels, hundreds of nanograms adequately deposited on a reflector.[14] This ability allows TXRF to be a very versatile tool and a good complement to this kind of research. In general, TXRF sensitivities are in the low parts per billion (ppb, or nanograms per milliliter) order, especially for gold quantification. This detection limit cannot compete with the sensitivity of ICP-MS, which is on the order of parts per trillion (ppt, or picograms per milliliter), but the combination of sensitivity and microanalytical character gives TXRF an analytical versatility that can help to solve many problems that, for other techniques, will be very difficult to solve. This work describes how TXRF, with its limitations and virtues, can evaluate GNP bioaccumulation in a relatively easy way. These facts confirm that TXRF spectrometry is a good alternative and versatile tool for researchers in this area.

TXRF is an original variation of conventional X-ray fluorescence (XRF) spectrometry.[14] Due to its special excitation geometry, in which the incidence angle of X-rays is below the critical angle of the reflector material, the incident X-ray beam is totally reflected from the surface. As a result, the sample placed in the center of the highly polished reflector is excited by the incident and the reflected beam through the X-ray standing wave field generated by the constructive interference of both. Because almost no penetration of the primary radiation in the reflector occurs, matrix effects and scattering are minimized, resulting in a significant improvement of the signal/background ratio that improves by around 3 orders of magnitude the absolute detection limits (few picograms) compared with conventional XRF. TXRF is a well-known technique[15] that has been more and more applied in very diverse scientific fields. Many applications has been developed up to now, including nanoparticle characterization,[16,17] catalytic processes studies,[18−20] medicine and biology,[21−26] physics of materials,[27−30] archaeometry,[31−34] forensics,[35] industrial applications,[36−38] and many others.

In this study, TXRF spectrometry has been applied for the first time to evaluate the bioaccumulation and clearance of gold nanorods (GNRs) at different times after intravenous administration in mice. Gold concentration was evaluated in various organs such as liver, spleen, brain, and lung and additionally in urine.

MATERIALS AND METHODS

Animals and Gold Nanorod Delivery. Male C57/BL6 mice, 9 months old, were used for the experiments. The mice had free access to food and water and were maintained on a 12 h dark/light cycle in a room with controlled temperature (25 ± 2 °C). Poly(ethylene glycol)-treated (PEGylated) GNRs (40 nm × 10 nm; Nanoseedz) were injected intravenously in mice at a dose of 4 μg/g in 200 μL of saline, a concentration that is routinely used to direct the particles to their targets in colloidal gold-based nanomedicine experiments designed for future medical applications.[39,40] The body weight of animals and their behavior were carefully recorded daily during the course of the experiment. The animals were injected and euthanized in accordance with the ethical guidelines for animal experimentation of Polytechnic University of Madrid by authorized staff. Experiments were carried out according to the Ethical Guidelines of the European Community (Directive 86/609/ECC).

Tissue Preparation for TXRF Analysis. Gold nanorod bioaccumulation kinetics were evaluated in liver, spleen, brain, and lung at 0 h, 1 h, 1 day, 1 week, and 1 month after GNR administration. Additionally, urine samples were obtained from mice to check the kinetics of elimination of GNRs by this excretion route. At the specified times, the animals were anesthetized with an overdose of chloral hydrate and intracardially perfused with freshly prepared buffered 4% paraformaldehyde (in 0.1 M phosphate buffer, pH 7.4). Organs were removed after animal perfusion, postfixed for 12 h in the same fixative at 4 °C, and dehydrated in 30% sucrose solution at 4 °C until sunk and were preserved at −20 °C. For all tissues, 10−70 mg aliquots of lyophilized samples were weighed in sterile polypropylene vials of 2 mL with cover. The digestion protocol was initiated by adding 1 mL of aqua regia (HCl/HNO_3, 3:1). Samples were standardized with 1 μg/g As (PlasmaCAL monoelemental certificate standard from SCP Science) as internal standard. Due to the high reactivity of the samples, the digestion process steps were as follows: orbital agitation for 2 h, short ultrasound exposition, and then lixiviation of the same on a hot plate. Samples were heated to 90 °C for 2 h and then were concentrated to a volume of 500 μL. To optimize and achieve the complete digestion of tissues, 10−20 μL of H_2O_2 and 500 μL of HNO_3, were added. All the reagents used in this work were of Suprapur trace metal grade from Fisher Scientific. The samples were heated again to 90 °C for 1 h and then concentrated to a volume around 100 μL, which implies a total concentration factor of 10. This step was the key to the sample preparation method due to the elimination of organic matter and, simultaneously, the concentration of metal contents. The developed method was tested and optimized by means of bovine liver (BCR-185R) certified reference material. Lyophilized bovine liver (50 mg) was weighed and doped with 10 μg/g gold (PlasmaCAL monoelemental certificate standard from SCP Science). In addition, each bovine liver sample was standardized with 1 μg/g As as internal standard. After complete digestion of the samples, 5 μL of each prepared sample was deposited onto a preheated quartz reflector and dried over a hot plate at 120 °C. In these conditions, samples were analyzed by TXRF. The

dx.doi.org/10.1021/ac5006475 | Anal. Chem. XXXX, XXX, XXX−XXX

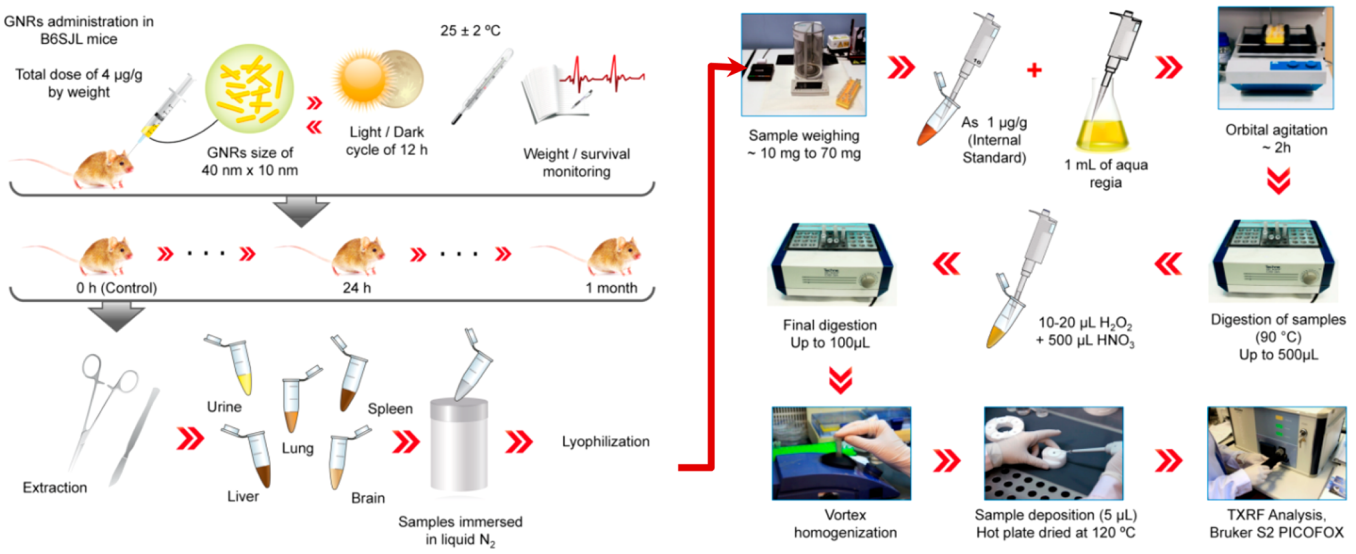

Figure 1. Animals, gold nanorod (GNR) delivery, and sample preparation protocol for TXRF.

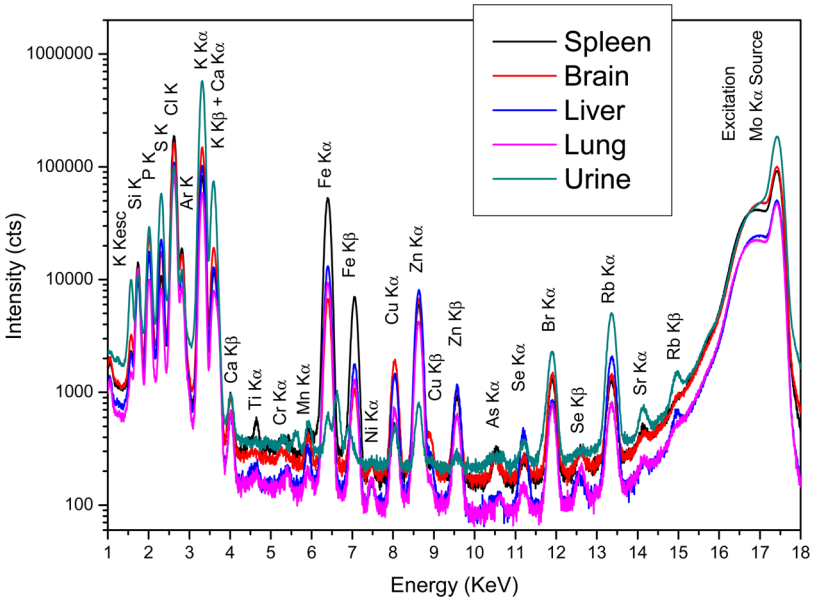

Figure 2. TXRF spectra of lixiviated blanks associated with each of the mouse tissues investigated; spleen, brain, liver, lung, and urine.

preparation protocol used for bovine liver was the same as used for the mouse samples and is graphically summarized in Figure 1.

TXRF Instrumentation. TXRF analysis of the samples was performed with a benchtop S2 PicoFox TXRF spectrometer from Bruker Nano GmbH (Germany), equipped with a molybdenum X-ray source working at 50 kV and 600 μA, a multilayer monochromator with 80% reflectivity at 17.5 keV (Mo Kα), an XFlash SDD detector with an effective area of 30 mm^2, and an energy resolution better than 150 eV for Mn Kα. Additionally the spectrometer was equipped with an automatic sample charger for 25 samples. The Spectra 7 software package, also from Bruker, was used for control, acquisition, deconvolution, and integration of all analyzed samples.

RESULTS AND DISCUSSION

Mouse Monitoring. After administration of GNRs, animals were examined daily for survival and evident behavioral or motor impairments. Mice were also weighed every day. To examine morphological changes, the brain, lungs, liver, and spleen were removed and weighed. We observed no mortality or any gross behavioral changes in mice receiving GNRs at the dose studied. No effect of GNR treatment on body weight was observed. Tissue size, color, and morphologies also remain unchanged after treatment with GNRs. No evidence of atrophy or inflammation was observed.

Qualitative Approximation. TXRF spectrometry allows simultaneous multielemental evaluation of the problem investigated. Figure 2 shows the TXRF spectra associated of all the blank lixiviated tissues investigated in this work. With the aim to maximize the signals associated with traces and simultaneously to minimize the strong signals of the major elements, a logarithmic scale for the intensity axis was applied.

It can be seen that the elemental fingerprints obtained for all the tissues were similar but with different elemental ratios. The TXRF spectra show characteristic X-ray transitions of the

dx.doi.org/10.1021/ac5006475 | Anal. Chem. XXXX, XXX, XXX−XXX

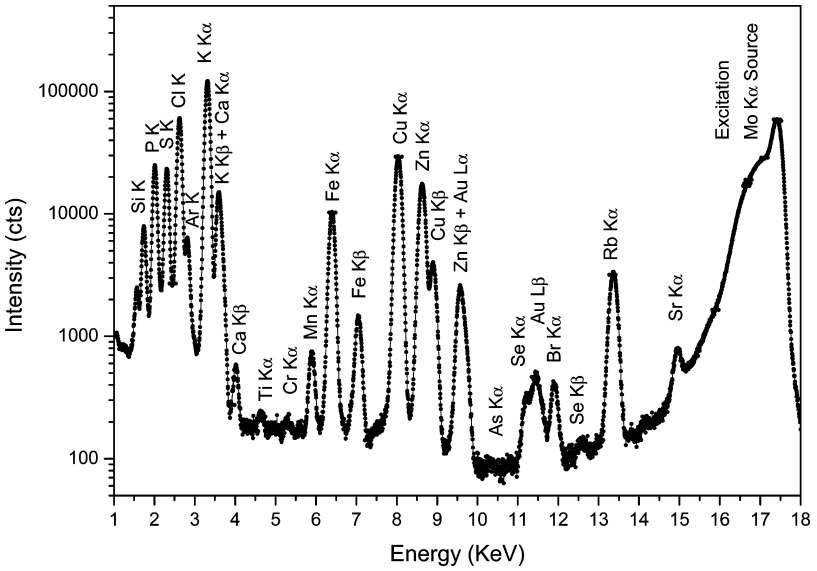

Figure 3. TXRF spectra of lixiviated bovine liver reference material (BCR-185R) doped with 10 μg/g Au.

following elements: P, S, Cl, K, Ca, Ti, Cr, Mn, Fe, Ni, Cu, Zn, As, Se, Br, Rb, and Sr. Furthermore, Si and Ar lines are not from the sample. Si comes from the quartz reflector on which the sample is deposited, and Ar comes from the atmospheric air because measurements are not performed in vacuum. Finally, the strong peak around 17 keV is due to the elastic (Mo Kα) and inelastic (Compton) scattering of the primary X-ray source used for exciting the atoms presents in the sample.

With the aim of simulating GNR bioaccumulation in a tissue, a reference material of bovine liver (BCR-185R) was doped with 10 μg/g Au. Figure 3 show the TXRF spectrum obtained after acid digestion.

In this case, the TXRF chemical fingerprint associated with the BCR-185R bovine liver reference material was similar to those obtained for all the other tissues (see Figure 2). The presence of Au signals corresponds to the element that was added as dopant. In the region where Au L-lines appear, Zn, Se, and Br lines are also present, from the bovine liver matrix, which have a strong overlap with Au L-lines. This is the case of the Zn Kβ line that overlaps with Au Lα and Se Kα that overlaps with Au Lβ. In any case, the right asymmetry observed in the Zn Kβ peak due to the Au Lα contribution and the clear peak observed for the Au Lβ line clearly ensures the presence of 10 μg/g Au added to the reference material as dopant.

An element used as internal standard for TXRF must fulfill several conditions: first and fundamentally, the element is not present in a meaningful way and with quantitative weight in the problem sample; second, the overlapping of its peaks with other elements present in the sample is minimal; third, the energy position of the main peak of the element is near the main peaks of the elements of interest (gold in our case); and finally, the order of concentration of the internal standard is in the average range of concentration of the elements of interest in the sample. So, following these basic rules based in our own experience, we selected arsenic (As) to standardize all the tissues investigated, even taking into account its presence in all evaluated tissues (see Figures 2 and 3). The maximum magnitude of As induction by the blanks was a few tens of parts per billion. Since the concentration of As added as internal standard has been 1 ppm (μg/mL), that is, 1000 ppb (ng/mL), the deviation in the nominal value of the standard concentration can be considered negligible, being around values ranging between 0.1% and 1%, which are far below the expanded uncertainty obtained in this study.

Once the complete set of elements was defined, this set was always applied for deconvolution, integration, and quantification in all analyzed samples.

Evaluation of Analytical Parameters. One of the first objectives of this study was to evaluate the virtues and drawbacks that TXRF can offer in this kind of research. Therefore, the developed acid digestion protocol and the TXRF measurements were extensively checked by determining the following analytical parameters: accuracy of the process by evaluating the gold recovery, average detection limits, and finally, global process precision by evaluating the uncertainty with a cover factor of $k = 2$ (95%).[41] A bovine liver certified reference material (BCR-185R) doped with 10 μg/g Au was used to test the developed methodology by TXRF. Five doped samples of BCR-185R were prepared in parallel following the protocol previously described under Tissue Preparation for TXRF Analysis. Table 1 shows the results achieved for the five samples of bovine liver reference material analyzed.

The analytical parameters achieved for TXRF Au measurements were as follows. The achieved average recovery of 99.7% with an expanded uncertainty of 5.6% indicates that the developed methodology by TXRF is very robust and accurate

Table 1. Concentration of Gold Obtained after Digestion and Analysis by TXRF[a]

sample[a]	Au[b] (μg/mL)	Au (μg/g)	recovery (%)	DL[b] (ng/mL)	DL (ng/g)
BCR1	0.513	10.178	102.6	6	119
BCR2	0.475	9.281	95.0	4	78
BCR3	0.501	9.839	100.2	4	79
BCR4	0.502	10.010	100.4	5	100
BCR5	0.502	10.012	100.4	9	179
		Statistical Parameters			
mean		9.86	99.7	6	111
$U_{k=2}$ (%)		7.00	5.6		

[a]Five bovine liver (BCR-185R) certified reference material samples were doped with 10 μg/g Au. [b]In solution. DL = detection limit.

dx.doi.org/10.1021/ac5006475 | Anal. Chem. XXXX, XXX, XXX−XXX

for the measurement of Au in this kind of matrix. Average detection limits of 6 ng/mL Au in solution and 111 ng/g Au in lyophilized liver tissue assure an adequate analytical potentiality of TXRF spectrometry for this kind of research. Finally, the reproducibility of the global analytical process was evaluated by calculating the expanded uncertainty of the process with a cover factor of $k = 2$, which implies a 95% success probability as shown by Fernandez-Ruiz.[41] The achieved global uncertainty of the Au TXRF measurement was 7.0%, which is the best expression of global precision of the developed analytical TXRF methodology.

In order to evaluate only the contribution of the instrumental TXRF measurements to the global precision of the developed methodology, the repeatability of the method was calculated. For this purpose, one of the BCR deposited samples, BCR3, was analyzed five times (n = 5) under the same measuring conditions but with the position of the quartz reflector rotated to include the influence of deposition inhomogeneities. In these conditions, the expanded uncertainty ($k = 2$) was only 1.7%, which is the best measure of the TXRF instrumental contribution to the global precision of the procedure. As a result, only 24.2% of the global uncertainty is due to the TXRF measurements and the remaining 75.8% is due to sample preparation.

Finally, the multielemental capability of the TXRF technique was evaluated by comparing the analytical parameters obtained for four additional elements of the BCR-185R reference material: Cu, Zn, Se, and Mn. In this way, recoveries, detection limits, and expanded uncertainties for $n = 5$ were also calculated in the same way as for Au.[41] These results are summarized in Table 2.

Table 2. Comparison of Analytical Results for Cu, Zn, Se, and Mn[a]

element	BCR value (μg/g)	avg concn (μg/g)	recovery (%)	DL[b] (ng/mL)	DL (ng/g)	$U_{k=2}$[c] (%)
Cu	277	251.4	90.8	7	139	7.4
Zn	138.6	138.5	101.1	5.4	107	7.9
Se	1.68	1.27	73.4	3.8	75	21.9
Mn	11.07	13.5	113.5	14	277	22.5

[a]Obtained from five ($n = 5$) bovine liver (BCR-185R) samples with certified values. [b]In solution. DL = detection limit.[c]. [c]U = expanded uncertainty.

In this case, for TXRF concentrations ranging from 1.27 μg/g for Se to 251.4 μg/g for Cu, expanded uncertainties vary from around 22% for Se and Mn, which are present in low concentrations, to around 7.7% for Cu and Zn, which are present in higher concentrations. Achieved recoveries vary from 73.4% for Se to 113.5% for Mn and the average recovery was 94.7%, which confirms the ability of the digestion method to evaluate not only Au but also additional metals present in the tissues. Detection limits ranged from 3.8 ng/mL for Se to 14 ng/mL for Mn in solution and from 75 ng/g for Se to 277 ng/g for Mn in lyophilized tissue. TXRF spectrometry has shown again its multielemental character by obtaining similar analytical parameters for the elements Cu, Zn, Se, and Mn as for Au.

Measurement of Bioaccumulation Kinetics of Au. Once the analytical procedure developed for TXRF was optimized, it was applied to study Au bioaccumulation kinetics of the mammalian tissues investigated. Figure 4 shows clearly

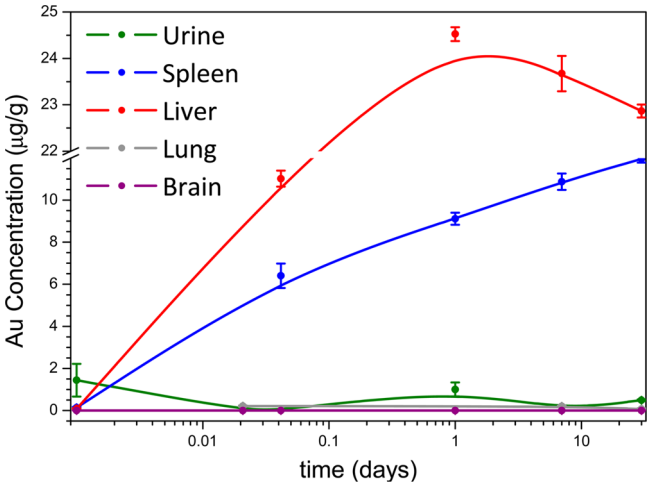

Figure 4. Gold nanorod bioaccumulation kinetics in spleen, liver, lung, brain, and urine. Error bars represent the expanded uncertainty $U_{k=2}$ of Au measured by TXRF.

two kinds of behavior. First, GNRs were quickly bioaccumulated by liver and spleen while they were not bioaccumulated in brain and lung for the time period investigated. The liver and spleen, which belong to the reticuloendothelial system, are mainly responsible for removal of different-sized particles, and hence these organs absorb a large percentage of systemically administered nanoparticles.[9] Most biodistribution studies have shown that approximately 50%−60% of the injected dose of nanoparticles is taken up by the liver and spleen, respectively.[9,41]

In our study, in the case of the liver, a change of slope is observed at 1 day after GNR injection. Additionally, only around 10% of GNRs are eliminated 1 month after injection. These results are consistent with those described in the literature, in which an accumulation of particles is shown in the liver even 1 month after administration,[5,42,43] indicating that gold particles are taken up by both hepatocytes and Kupffer cells in the liver and cleared by the hepatobiliary system and later through the Kupffer cells via an unknown mechanism.[39] In the case of spleen and during the period of time evaluated, the slope of the observed kinetics was always positive, suggesting that GNRs were also trapped in spleen macrophages and thus indicating clearance of PEG-coated GNRs at a slow pace.[43]

The absence of GNRs in the brain samples analyzed is fully in line with published data, showing that penetration of GNPs across the blood−brain barrier is critically size-dependent with an upper penetration limit of about 15−20 nm.[2] In parallel, urine also shows an absence of GNR accumulation, only with small oscillations around the background, indicating that these GNRs are not eliminated via urine; only 2 nm nanoparticles can be excreted via urine.[41]

In the recent work of Goel et al.,[39] high concentrations of GNRs have been also observed in the liver and spleen 24 h after intravenous injection and showing no significant changes for nearly 4 months. Our results confirm these results and show that GNRs are mainly accumulated in liver and spleen at both 24 h and 1 month after injection. It is well-know that liver and spleen are highly vascular filtration organs. That is why it is not surprising that these organs collect and bioaccumulate large amount of GNRs in their tissues. The long-time retention and slow clearance of GNRs from organs of the reticuloendothelial system shown in this research (Figure 3) closely resembles the

dx.doi.org/10.1021/ac5006475 | Anal. Chem. XXXX, XXX, XXX−XXX

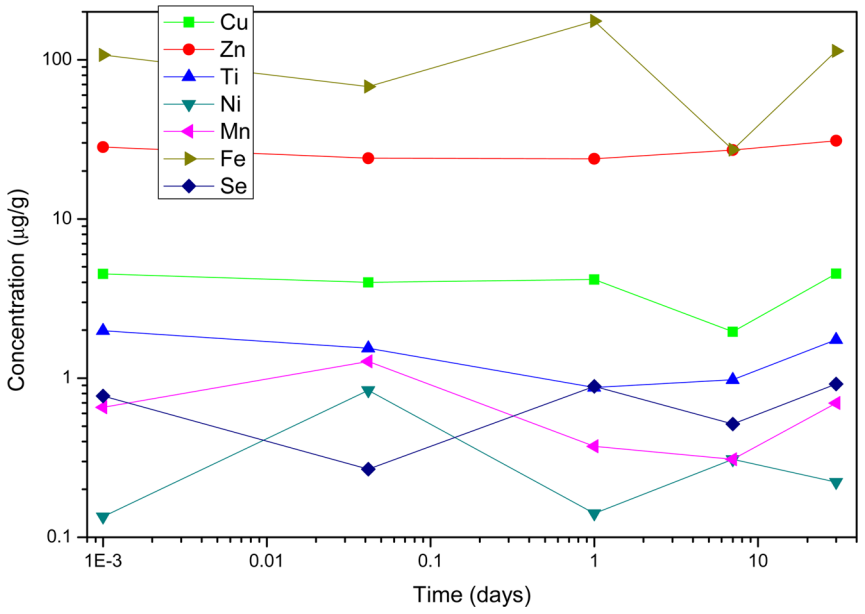

Figure 5. Elemental concentrations of Cu, Zn, Ti, Ni, Mn, Fe, and Se over time for liver.

slow clearance of nanorods described by Wang et al.[5] As the excretion of accumulated particles from the liver and spleen can take up to 3−4 months,[40] the question about injected doses and possible inflammation processes is still of great importance.[44] Due to the slow rate of clearance of GNRs from organs of the reticuloendothelial system, further long-term in vivo studies are needed to determine the GNR biodistribution, accumulation, retention, and clearance effects and their role in toxicity before exposure of humans to this kind of nanoparticles useful in future biomedical applications.

Evaluation of Biological Variability. When a complex system is modified by the addition or elimination of an element, the system usually re-equilibrates the elemental composition to reach equilibrium again. In this way, analytical techniques, such as TXRF, that can study complex systems from a global and multielemental point of view should be of high interest for the study of elemental intercorrelations in each investigated problem. In this case and with the aim of evaluating more deeply the multielemental capabilities of TXRF to characterize these kind of tissues, and additionally to check the existence of elemental correlations with the bioaccumulation behavior found for GNPs, an estimation (n = 5) of the biological variability of the elements Cu, Zn, Ti, Ni, Mn, Fe, and Se was made. With the controlled life conditions of the mice used during the month of the experiment taken into account, the aforementioned elements were simultaneously quantified in the same way as Au from GNRs. Figure 5 shows that, in the case of liver, the element behaviors were random around their mean values along time. These findings were similar for all other investigated tissues: spleen, lung, and brain. In conclusion, for all the elements evaluated, correlations were not found due to the anomalous presence of GNRs in the mice.

Once the absence of correlations was observed, the biological variability of the elements Cu, Zn, Ti, Ni, Mn, Fe ,and Se in each of the investigated tissues was evaluated with the aim to check the multielemental character of TXRF. Statistical analysis of the variations found for the five samples analyzed from each tissue allows a first estimation of their elemental biological variability. Table 3 shows the obtained results for each tissue investigated: average concentration, standard deviation σ for k = 1, and coefficient of variation (CV) for each of the elements evaluated.

Table 3. Biological Variability Obtained for Cu, Zn, Ti, Ni, Mn, Fe, and Se Concentrations (n = 5) in Liver, Brain, Lung, and Spleen Tissue Samples

	tissue			
	liver	brain	lung	spleen
		Cu		
avg concn (μg/g)	3.83	7.00	3.92	2.45
σ (μg/g)	1.08	2.79	1.86	0.89
CV (%)	28.05	39.81	47.32	36.32
		Zn		
avg concn (μg/g)	26.84	41.30	17.82	43.61
σ (μg/g)	3.01	18.17	5.49	15.86
CV (%)	11.22	44.00	30.81	36.36
		Ni		
avg concn (μg/g)	0.33	0.21	0.12	0.55
σ (μg/g)	0.29	0.09	0.05	0.38
CV (%)	89.07	41.26	46.77	68.65
		Mn		
avg concn (μg/g)	0.66	1.13	0.69	2.36
σ (μg/g)	0.38	0.72	0.29	1.42
CV (%)	57.72	63.25	41.51	60.43
		Fe		
avg concn (μg/g)	98.06	28.81	60.74	417.79
σ (μg/g)	55.16	15.62	27.28	257.81
CV (%)	56.26	54.24	44.92	61.71
		Ti		
avg concn (μg/g)	1.42	2.23	0.92	7.14
σ (μg/g)	0.48	1.43	0.41	6.96
CV (%)	33.97	64.12	45.10	97.40
		Se		
avg concn (μg/g)	0.58	0.22	0.19	0.32
σ (μg/g)	0.39	0.12	0.05	0.24
CV (%)	68.09	57.14	27.07	76.16

Figure 6 shows the elemental quantitative fingerprint for each of the tissues investigated in this work, with standard deviations

dx.doi.org/10.1021/ac5006475 | Anal. Chem. XXXX, XXX, XXX−XXX

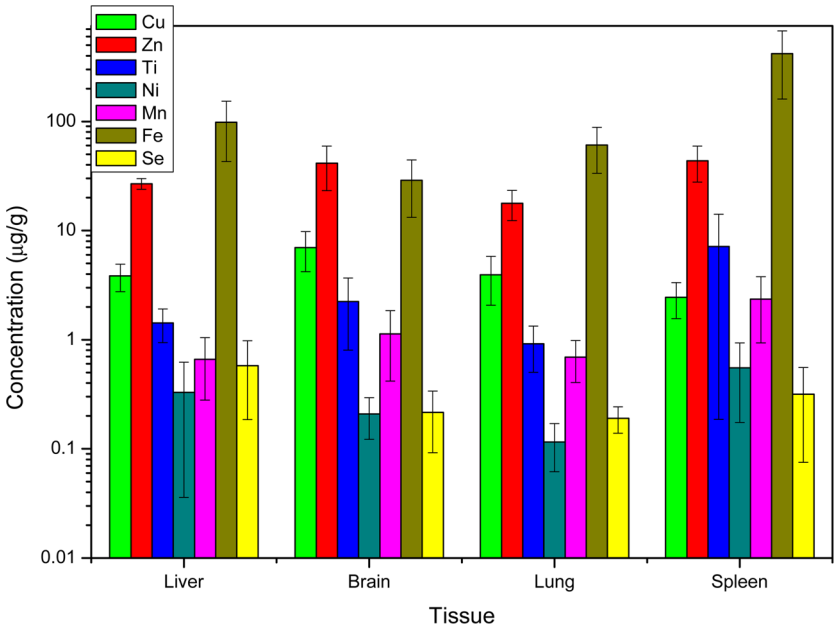

Figure 6. Elemental quantitative fingerprint for liver, brain, lung, and spleen tissues with standard deviations for each element evaluated.

for each of the elements evaluated (Cu, Zn, Ti, Ni, Mn, Fe, and Se) represented as error bars. As can be seen, no significant differences, within error, were found when the elemental concentrations were compared between tissues, with the exception of the high Fe level present in spleen. Also in the spleen, we observed a change in the balance of Cu and Ti (Cu < Ti), while in the other tissues the balance is the opposite (Cu > Ti). The rest of the parameters display very similar ratios and trends.

CONCLUSIONS

To the best of our knowledge, this study is the first application of TXRF spectrometry as an analytical method to evaluate low concentrations of GNRs in several tissues and also one of the first systematic studies of GNR bioaccumulation kinetics in vital mammalian organs of mice at long time periods (longer than 1 month) after administration. The kinetics of bioaccumulation of GNRs showed two different behaviors, with liver and spleen being the dominant targeted organs while brain, lungs, and urine did not show any significant GNR accumulation. It is necessary to study GNR accumulation for longer periods of time due to their health implications and possible side effects. TXRF spectrometry has been demonstrated to be a powerful and accurate analytical alternative technique to the conventional techniques used up to now for GNP quantification, such as ICP-MS, atomic absorption spectroscopy (AAS), INAA, and radioactive analysis (RA). The low cost and quick analysis in addition to high accuracy, high precision, and low detection limits confirm that TXRF is a solid analytical technique to develop high-quality research in bioaccumulation studies of gold nanorods in particular and metal nanoparticles in biological systems in general.

AUTHOR INFORMATION

Corresponding Author

*Fax +34 914973529; e-mail ramon.fernandez@uam.es..

Notes

The authors declare no competing financial interest.

ACKNOWLEDGMENTS

We acknowledge financial support from Universidad Autónoma de Madrid and Comunidad de Madrid by the EIADES S2009/AMB 1478 project and by the Foundation Reina Sofía. Also, we thank Marta González Mella (Animal Facility Center of CBMSO, UAM-CSIC) for her valuable ideas and technical support.

REFERENCES

(1) Dreaden, E. C.; Alkilany, A. M.; Huang, X.; Murphy, C. J.; El-Sayed, M. A. *Chem. Soc. Rev.* **2012**, *41* (7), 2740−79.
(2) Dykman, L.; Khlebtsov, N. *Chem. Soc. Rev.* **2012**, *41* (6), 2256−82.
(3) Wu, D.; Zhang, X. D.; Liu, P. X.; Zhang, L. A.; Fan, F. Y.; Guo, M. L. *Curr. Nanosci.* **2011**, *7*, 110−118.
(4) Hu, M.; Chen, J.; Li, Z. Y.; et al. *Chem. Soc. Rev.* **2006**, *35*, 1084−1094.
(5) Wang, L.; Li, Y. F.; Zhou, L.; Liu, Y.; Meng, L.; Zhang, K.; Wu, X.; Zhang, L.; Li, B.; Chen, C. *Anal. Bioanal. Chem.* **2010**, *396* (3), 1105−1114.
(6) Grobmyer, S. R., Moudgil, B. M., Eds. *Cancer Nanotechnology: Methods and Protocols*; Springer: New York, 2010.
(7) Sonavane, G.; Tomoda, K.; Makino, K. *Colloids Surf. B: Biointerfaces* **2008**, *66* (2), 274−280.
(8) Niidome, T.; Yamagata, M.; Okamoto, Y.; Akiyama, Y.; Takahashi, H.; Kawano, T.; Katayama, Y.; Niidome, Y. *J. Controlled Release* **2006**, *114*, 343−347.
(9) De Jong, W. H.; Hagens, W. I.; Krystek, P.; Burger, M. C.; Sips, A. J.; Geertsma, R. E. *Biomaterials* **2008**, *29*, 1912−1919.
(10) Hirn, S.; Semmler-Behnke, M.; Schleh, C.; Wenk, A.; Lipka, J.; Schäffler, M.; Takenaka, S.; Möller, W.; Schmid, G.; Simon, U.; Kreyling, W. G. *Eur. J. Pharm. Biopharm.* **2011**, *77* (3), 407−416.
(11) Sadauskas, E.; Wallin, H.; Stoltenberg, M.; Vogel, U.; Doering, P.; Larsen, A.; Danscher, G. *Part. Fibre Toxicol.* **2007**, *4*, 10.
(12) Darien, B. J.; Sims, P. A.; Kruse-Elliott, K. T.; Homan, T. S.; Cashwell, R. J.; Cooley, A. J.; Albrecht, R. M. *Scanning Microsc.* **1995**, *9* (3), 773−780.
(13) Erickson, T.; Tunnell, J. W. In *Mixed Metal Nanomaterials*; Nanomaterials for the Life Sciences, Vol. 3; Kumar, C. S. S. R., Ed.; Wiley−VCH: Weinheim, Germany, 2009.
(14) Yoneda, Y.; Horiuchi, T. *Rev. Sci. Instrum.* **1971**, *42*, 1069−1070.

(15) Klockenkäper, R. *Total-Reflection X-ray Fluorescence Analysis*; John Wiley & Sons Inc.: New York, 1997.
(16) Fernández-Ruiz, R.; Costo, R.; Morales, M. P.; Bomatí-Miguel, O.; Veintemillas-Verdaguer, S. *Spectrochim. Acta, Part B* **2008**, *63*, 1387−1394.
(17) Fernández-Ruiz, R.; Ocon, P.; Montiel, M. *J. Anal. At. Spectrom.* **2009**, *24*, 785−791.
(18) Fernández-Ruiz, R.; Furió, M.; Cabello Galisteo, F.; Larese, C.; López Granados, M.; Mariscal, R.; Fierro, J. L. G. *Anal. Chem.* **2002**, *74* (21), 5463−5469.
(19) Fernández-Ruiz, R.; Cabello Galisteo, F.; Larese, C.; López Granados, M.; Mariscal, R.; Fierro, J. L. G. *Analyst* **2006**, *131*, 590−594.
(20) Fernández-Ruiz, R.; Rodríguez-Ubis, J. C.; Salvador, A.; Brunet, E.; Juanes, O. *J. Anal. At. Spectrom.* **2010**, *25*, 1882−1887.
(21) Fernández-Ruiz, R.; Tornero, J. D.; González, V. M.; Alonso, C. *Analyst* **1999**, *124*, 583−585.
(22) González, M.; Tapia, L.; Alvarado, M.; Tornero, J. D.; Fernández-Ruiz, R. *J. Anal. At. Spectrom.* **1999**, *14*, 885−888.
(23) Magalhães, T.; von Bohlen, A.; Carvalho, M. L.; Becker, M. *Spectrochim. Acta, Part B* **2006**, *61*, 1185−1193.
(24) Fernández-Ruiz, R.; Malki, M.; Morato, A. I.; Marin, I. *J. Anal. At. Spectrom.* **2011**, *26*, 511−516.
(25) Zarkadas, Ch.; Karydas, A. G.; Paradellis, T. *Spectrochim. Acta, Part B* **2001**, *56* (11), 2219−2228.
(26) Zarkadas, Ch.; Karydas, A. G.; Paradellis, T. *Spectrochim. Acta, Part B* **2001**, *56* (12), 2505−2511.
(27) Fernández-Ruiz, R.; Capmany, J. *J. Anal. At. Spectrom.* **2001**, *16*, 867−869.
(28) Fernández-Ruiz, R.; Cabañero, J. P.; Hernández, E.; León, M. *Analyst* **2001**, *126*, 1797−1799.
(29) Krämer, M.; von Bohlen, A.; Sternemann, C.; Paulus, M.; Hergenröder, R. *Appl. Surf. Sci.* **2007**, *253* (7), 3533−3542.
(30) Zheng, Q.; Dierre, F.; Corregidor, V.; Fernández-Ruiz, R.; Crocco, J.; Bensalah, H.; Alves, E.; Diéguez, E. *J. Cryst. Growth* **2012**, *358*, 89−93.
(31) García-Heras, M.; Fernández-Ruiz, R.; Tornero, J. D. *J. Archaeol. Sci.* **1997**, *24* (11), 1003−1014.
(32) Von Bohlen, A. *Anal. Lett.* **2004**, *37*, 491−498.
(33) Fernández-Ruiz, R.; García-Heras, M. *Spectrochim. Acta, Part B* **2007**, *62*, 1123−1129.
(34) Fernández-Ruiz, R.; García-Heras, M. *Spectrochim. Acta, Part B* **2008**, *63*, 975−979.
(35) Ninomiya, T.; Nomura, S.; Taniguchi, K.; Ikeda, S. *Adv. X-ray Chem. Anal., Jpn.* **1994**, *26*, 9−18.
(36) Ojeda, N.; Greaves, E. D.; Alvarado, J.; Sajo-Bohus, L. *Spectrochim. Acta, Part B* **1993**, *48* (2), 247−253.
(37) Carvalho, M. L.; Barreiros, M.; Costa, M.; Ramos, M.; Marques, M. *X-Ray Spectrom.* **1996**, *25*, 29−32.
(38) Haswell, S. J.; Walmsley, A. D. *J. Anal. At. Spectrom.* **1998**, *13*, 131−134.
(39) Goel, R.; Shah, N.; Visaria, R.; Paciotti, G. F.; Bischof, J. C. *Nanomedicine* **2009**, *4* (4), 401−410.
(40) Khlebtsov, N.; Dykman, L. *Chem. Soc. Rev.* **2011**, *40* (3), 1647−1671.
(41) Fernández-Ruiz, R. *Anal. Chem.* **2008**, *80* (22), 8372−8381.
(42) Cho, W. S.; Cho, M.; Jeong, J.; Choi, M.; Cho, H. Y.; Han, B. S.; Kim, S. H.; Kim, H. O.; Lim, Y. T.; Chung, B. H.; Jeong, J. *Toxicol. Appl. Pharmacol.* **2009**, *1, 236* (1), 16−24.
(43) Lasagna-Reeves, C.; Gonzalez-Romero, D.; Barria, M. A.; Olmedo, I.; Clos, A.; Sadagopa Ramanujam, V. M.; Urayama, A.; Vergara, L.; Kogan, M. J.; Soto, C. *Biochem. Biophys. Res. Commun.* **2010**, *19, 393* (4), 649−55.
(44) Dykman, L.; Khlebtsov, N. *Chem. Soc. Rev.* **2012**, *21, 41* (6), 2256−82.